7

INHOMOGENEITIES

Having set up the system of equations to be solved and the initial conditions for the perturbations, we can now calculate the inhomogeneities and anisotropies in the universe. In this first solutions chapter, we start with the perturbations to the dark matter. In principle these are coupled to all other perturbations. In practice, though, perturbations to the dark matter depend very little on the details of the radiation perturbations. Dark matter, by definition, is affected by radiation only indirectly, through the gravitational potentials. At late times, when the universe is dominated by matter, these potentials are independent of the radiation. At early times, while it is true that the potentials are determined by the radiation, it is also true that the radiation perturbations are relatively simple, so that all moments beyond the monopole and dipole can be neglected. The converse is not true, as we will see in the next chapter: To treat the anisotropies properly we will need to know how the matter perturbations behave.

The ultimate goal of this exercise is to compare theory with observations. We will solve for the evolution of each Fourier mode, $\delta(k, \eta)$. Given this solution, and the initial power spectrum generated by inflation, we can construct the power spectrum of matter today. At least on large scales, this is the most important observable. On small scales, comparison with observation today is more difficult: one must worry about nonlinearities and gas dynamics when comparing with the galaxy distribution. Nonetheless, even on small scales, the linear power spectrum, which we compute in this chapter, is often the starting point for any quantitative statement about the distribution of matter.

7.1 PRELUDE

Gravitational instability is a powerful idea, easy to understand, and most likely responsible for the structure in our universe. As time evolves, matter accumulates in initially overdense regions. It doesn't matter how small the initial overdensity was (e.g., in typical cosmological scenarios, the overdensity was of order 1 part in 10^5); eventually enough matter will be attracted to the region to form structure.

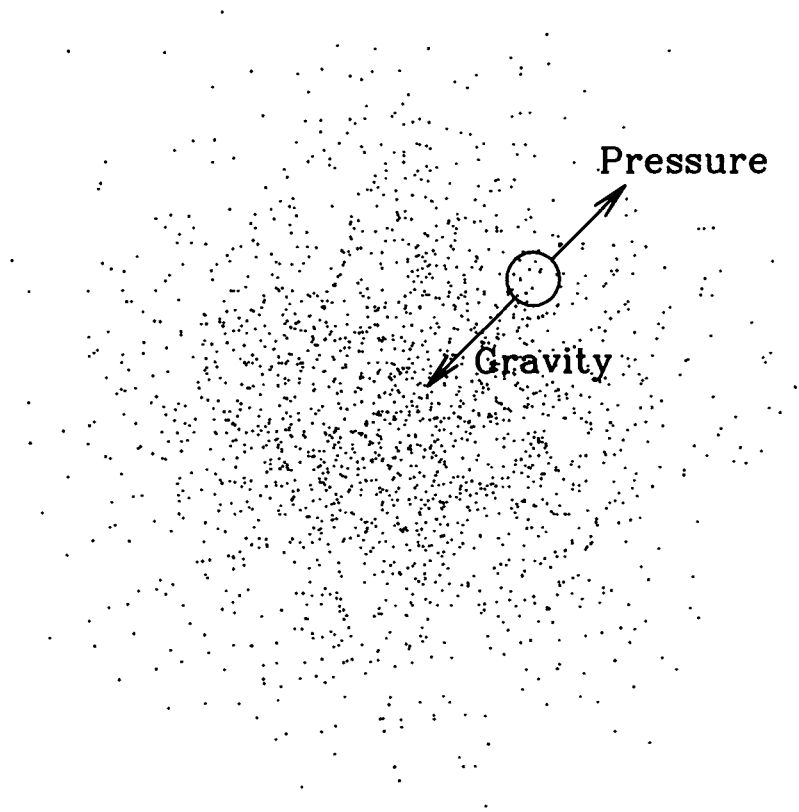

Figure 7.1. Gravitational instability. Mass near an overdense region is attracted to the center by gravity but repelled by pressure. If the region is dense enough, gravity wins and the overdensity grows with time.

The $F = ma$ of gravitational instability is the equation governing overdensities δ. Schematically, it reads

$$\ddot{\delta} + [\text{Pressure} - \text{Gravity}]\ \delta = 0. \tag{7.1}$$

These basic forces, depicted in Figure 7.1, act in opposite directions. Gravity acts to increase overdensities, grabbing more matter into the region. Since there are more particles in an overdense region, random thermal motion causes a net loss of mass in an overdense region. Therefore, if pressure is strong, inhomogeneities do not grow. As indicated by the cartoon equation (7.1), if pressure is low, δ grows exponentially; if it is large, δ oscillates with time.

We will see many manifestations of the simple form of gravitational instability depicted in Eq. (7.1). Different ambient cosmological conditions alter the growth rate. For example, in a matter-dominated universe, δ grows only as a power of time, not exponentially, whereas in a radiation-dominated universe, the growth is

but logarithmic. We will treat super-horizon versions of this equation as well as the more familiar sub-horizon version. When going though the math, though, it is useful to bear in mind the dueling concepts of gravity and pressure.

7.1.1 Three Stages of Evolution

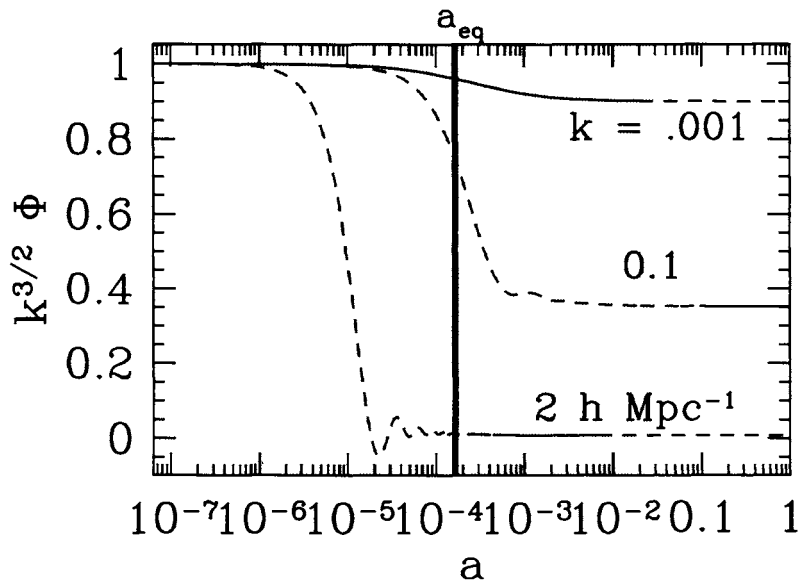

Figure 7.2. The linear evolution of the gravitional potential Φ. Dashed line denotes that the mode has entered the horizon. Evolution through the shaded region is described by the transfer function. The potential is unnormalized, but the relative normalization of the three modes is as it would be for scale-invariant perturbations. Here baryons have been neglected, $\Omega_m = 1$, and $h = 0.5$.

The evolution of cosmological perturbations breaks up naturally into three stages. To see this, let's cheat and look at the solutions for several different modes. Figure 7.2 shows the gravitational potential as a function of scale factor for long-, medium-, and short-wavelength modes. Early on, all of the modes are outside the horizon ($k\eta \ll 1$) and the potential is constant. At intermediate times (shaded in the figure), two things happen: the wavelengths fall within the horizon and the universe evolves from radiation domination ($a \ll a_{\rm eq}$) to matter domination ($a \gg a_{\rm eq}$). Without getting into the details, we see that the order of these epochs ($a_{\rm eq}$ and the epoch of horizon crossing) greatly affects the potential. The large-scale mode, which enters the horizon well after $a_{\rm eq}$, evolves much differently than the small-scale mode, which enters the horizon before equality. Finally, at late times, all the modes evolve identically again, in this case (where $\Omega_m = 1$) remaining constant.

We are able to observe the distribution of matter predominantly at late epochs, in the third stage of evolution, when all modes are evolving identically. If we wish to relate the potential during these times to the primordial potential set up during inflation, and we do, we can write schematically

$$\Phi(\vec{k}, a) = \Phi_{\rm p}(\vec{k}) \times \left\{\text{Transfer Function}(k)\right\} \times \left\{\text{Growth Function}(a)\right\}. \qquad (7.2)$$

where $\Phi_{\rm p}$ is the primordial value of the potential, set during inflation. The transfer function describes the evolution of perturbations through the epochs of horizon cossing and radiation/matter transition (the shaded region in Figure 7.2), while the growth factor describes the wavelength-independent growth at late times. This schematic equation is indeed roughly how the growth factor and the transfer function are defined, with two caveats, both due to convention. Notice from Figure 7.2 that even the largest wavelength perturbations decline slightly as the universe passes through the epoch of equality. This decline is conventionally removed so that the transfer function on large scales is equal to 1. Therefore, the transfer function is defined as

$$T(k) \equiv \frac{\Phi(k, a_{\rm late})}{\Phi_{\rm Large-Scale}(k, a_{\rm late})} \qquad (7.3)$$

where $a_{\rm late}$ denotes an epoch well after the transfer function regime and the *Large-Scale* solution is the primordial Φ decreased by a small amount. We will derive in Section 7.2 that — neglecting anisotropic stresses — this factor is equal to (9/10). The second caveat concerns the growth function. The ratio of the potential to its value right after the transfer function regime is defined to be

$$\frac{\Phi(a)}{\Phi(a_{\rm late})} \equiv \frac{D_1(a)}{a} \qquad (a > a_{\rm late}), \qquad (7.4)$$

where D_1 is called the growth function. In the flat, matter-dominated case depicted in Figure 7.2, then, the potential is constant so $D_1(a) = a$. With these conventions, we have

$$\Phi(\vec{k}, a) = \frac{9}{10}\Phi_{\rm p}(\vec{k})T(k)\frac{D_1(a)}{a} \qquad (a > a_{\rm late}). \qquad (7.5)$$

The easiest way to probe the potential is to measure the matter distribution. Figure 7.3 shows the evolution of the matter overdensity for three different modes. Notice that at late times — when the potential is constant and all the modes are within the horizon — the overdensity grows with the scale factor ($\delta \propto a$). This explains the seemingly odd nomenclature above (Why is it called a *growth* function if the potential remains constant?): D_1 describes the growth of the matter perturbations at late times. This growth is completely consistent with our intuition that as time evolves, overdense regions attract more and more matter, thereby becoming more overdense.

We can now express the power spectrum of the matter distribution in terms of the primordial power spectrum generated during inflation, the transfer function, and the growth function. The simplest way to relate the matter overdensity to the

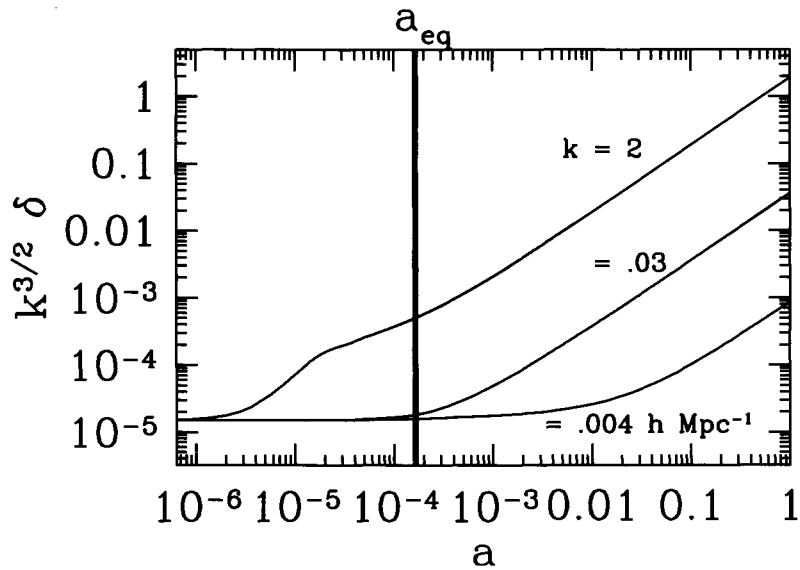

Figure 7.3. The evolution of perturbations to the dark matter in the same model as plotted in Figure 7.2. Amplitude starts to grow upon horizon entry (different times for the three different modes shown here). Well after $a_{\rm eq}$, all sub-horizon modes evolve identically, scaling as the growth factor. In the case plotted, a flat, matter dominated universe, the growth factor is simply equal to a.

potential at late times is to use Poisson's equation (the large-k, no-radiation limit of Eq. (5.81))

$$\Phi = \frac{4\pi G\rho_{\rm m}a^2\delta}{k^2} \qquad (a > a_{\rm late}). \tag{7.6}$$

The background density of matter is $\rho_{\rm m} = \Omega_m\rho_{\rm cr}/a^3$, and $4\pi G\rho_{\rm cr} = (3/2)H_0^2$, so

$$\delta(\vec{k},a) = \frac{k^2\Phi(\vec{k},a)a}{(3/2)\Omega_m H_0^2} \qquad (a > a_{\rm late}). \tag{7.7}$$

This, together with Eq. (7.5), allows us to relate the overdensity today to the primordial potential

$$\delta(\vec{k},a) = \frac{3}{5}\frac{k^2}{\Omega_m H_0^2}\Phi_{\rm p}(\vec{k})T(k)D_1(a) \qquad (a > a_{\rm late}). \tag{7.8}$$

Equation (7.8) holds regardless of how the initial perturbation $\Phi_{\rm p}$ was generated. In the context of inflation, $\Phi_{\rm p}(\vec{k})$ is drawn from a Gaussian distribution with mean zero and variance (Eq. (6.100)) $P_\Phi = (50\pi^2/9k^3)(k/H_0)^{n-1}\delta_H^2(\Omega_m/D_1(a=1))^2$. So the power spectrum of matter at late times is

$$P(k,a) = 2\pi^2\delta_H^2\frac{k^n}{H_0^{n+3}}T^2(k)\left(\frac{D_1(a)}{D_1(a=1)}\right)^2 \qquad (a > a_{\rm late}). \tag{7.9}$$

The power spectrum has dimensions of (length)^3. If we want to express the power as a dimensionless function, then, we must multiply by k^3. More precisely, one often associates $d^3kP(k)/(2\pi)^3$ with the excess power in a bin of width dk centered at k. After integrating over all orientations of $\vec{k}$, this becomes $(dk/k)\Delta^2(k)$, with

$$\Delta^2(k) \equiv \frac{k^3 P(k)}{2\pi^2}. \tag{7.10}$$

Small Δ then corresponds to small inhomogeneities, while large Δ indicates nonlinear perturbations. Note that, with our conventions, a Harrison–Zel'dovich–Peebles spectrum today has $\Delta^2 = \delta_H^2$ on a horizon-sized scale ($k = H_0$).

Figure 7.4 shows the power spectrum today for two different models. Note that in both of the models $P \propto k$ on large scales, where the transfer function is unity. This behavior is apparent from Eq. (7.9) and corresponds to the simplest inflationary model, wherein $n = 1$. On small scales the power spectrum turns over. To understand this, look back at Figure 7.2. The small-scale mode there ($k = 2\,h$ Mpc^{-1}) enters the horizon well before matter/radiation equality. During the radiation epoch the potential decays, so the transfer function is much smaller than unity. The effect of this on matter perturbations can be seen in Figure 7.3, where the growth of δ is retarded starting at $a \simeq 10^{-5}$ after the mode has entered the horizon and ending at $a \simeq 10^{-4}$ when the universe becomes matter dominated. Modes that enter the horizon even earlier undergo more suppression. Thus, the power spectrum is a decreasing function of k on small scales.

This leads to the realization that there will be a turnover in the power spectrum at a scale corresponding to the one which enters the horizon at matter/radiation equality. The power of this realization is apparent in Figure 7.4, which shows two different models: one corresponding to a flat, matter-dominated universe today (often called standard Cold Dark Matter or sCDM) and the other a universe with a cosmological constant today (Lambda Cold Dark Matter or ΛCDM). The major difference between the two models is that sCDM has more matter ($\Omega_m = 1$) and hence an earlier $a_{\rm eq}$. An earlier $a_{\rm eq}$ means only the very small scales enter the horizon during the radiation-dominated epoch, and therefore the turnover occurs on smaller scales. Finally, another important scale to keep in mind is the scale above which nonlinearities cannot be ignored. This is roughly set by $\Delta(k_{\rm nl}) \simeq 1$, which corresponds to $k_{\rm nl} \simeq 0.2\,h$ Mpc^{-1} in most models. The power spectra shown in Figure 7.4 are the linear power spectra today. On scales smaller than $k_{\rm nl}$, one cannot blindly compare the spectra from Figure 7.4 with the matter distribution today.

7.1.2 Method

What are the evolution equations for the dark matter overdensity? In principle, these are the full set of Boltzmann equations derived in Chapter 4 and the pair of Einstein equations from Chapter 5. In practice, though, the full set of equations is not needed. To understand why, recall that early on (before recombination at

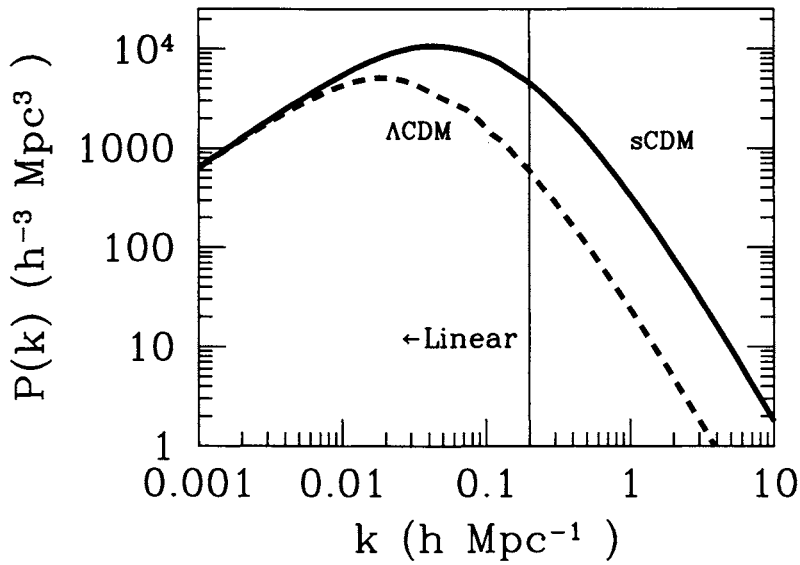

Figure 7.4. The power spectrum in two Cold Dark Matter models, with (ΛCDM) and without (sCDM) a cosmological constant. The spectra have been normalized to agree on large scales. The spectrum in the cosmological constant model turns over on larger scales because of a later $a_{\rm eq}$. Scales to the left of the vertical line are still evolving linearly.

$a = a_*$), the photon distribution can be characterized by only two moments, the monopole Θ_0 and the dipole Θ_1. All other moments are suppressed because the photons are tightly coupled to the electron/proton gas. After decoupling this ceases to be true, and to completely characterize the photon distribution we will need to follow high moments. However, for the purposes of the matter distribution, what the photons are doing after a_* is irrelevant. For, by that time, which is typically well into the matter era, the potential is dominated by the dark matter itself. To sum up then, we can neglect all photon moments except for the monopole and dipole when we are considering the evolution of the matter distribution.

Neglecting the higher radiation moments, the four relevant Boltzmann equations (Section 4.7) become

$$\dot{\Theta}_{r,0} + k\Theta_{r,1} = -\dot{\Phi} \tag{7.11}$$

$$\dot{\Theta}_{r,1} - \frac{k}{3}\Theta_{r,0} = \frac{-k}{3}\Phi \tag{7.12}$$

$$\dot{\delta} + ikv = -3\dot{\Phi} \tag{7.13}$$

$$\dot{v} + \frac{\dot{a}}{a}v = ik\Phi. \tag{7.14}$$

Even with the assumption that only the monopole and dipole are retained, getting

from Eq. (4.100) to Eqs. (7.11) and (7.12) requires some explanation and work. First, the explanation: The subscript $_r$ here refers to radiation, both neutrinos and photons. Both species contribute to the gravitational potential (which is our interest in this chapter) and both start out with the same initial conditions. It is not quite as obvious that both follow the same evolution equations (the $\dot{\tau}$ terms can be neglected in Eq. (4.100)) or that these evolution equations are the ones given in (7.11) and (7.12). But it is true, at least in the limit of small baryon density, and again only for the purposes of following the matter evolution. You can work out the details in Exercise 1, and we will explore the full photon evolution equation in the next chapter.

To close the set of equations for the dark matter density, we need an equation for the gravitational potential Φ. You may have noticed that in Eqs. (7.11)-(7.14), I set $\Psi \to -\Phi$, an approximation valid in the limit that there are no quadrupole moments (Eq. (5.33)). Since some of the Einstein equations are redundant, we have several choices for one last equation relating Φ to the radiation and matter overdensities. We can use the time-time component, Eq. (5.27),

$$k^2\Phi + 3\frac{\dot{a}}{a}\left(\dot{\Phi} + \frac{\dot{a}}{a}\Phi\right) = 4\pi G a^2 \left[\rho_{\rm dm}\delta + 4\rho_r\Theta_{r,0}\right]. \tag{7.15}$$

Here, again I have set Ψ to $-\Phi$, neglected the baryons,[1] and merged the neutrino and photon contributions to the potential. The alternative is to use the algebraic (no time derivatives) equation (5.81):

$$k^2\Phi = 4\pi G a^2 \left[\rho_{\rm dm}\delta + 4\rho_r\Theta_{r,0} + \frac{3aH}{k}\left(i\rho_{\rm dm}v + 4\rho_r\Theta_{r,1}\right)\right]. \tag{7.16}$$

Both of these equations will be useful to us at various times, although only one is necessary to close the set of equations for the five variables $\delta, v, \Theta_{r,0}, \Theta_{r,1}$, and Φ.

At this stage, the simplest thing to do is solve the set of five coupled equations numerically (Exercise 2). If Eq. (7.15) is used, there are no numerical difficulties, and with very little work, you can have a code which computes the transfer function (in the absence of baryons) in less than a second.

Analytic solutions for the dark matter density are harder to come by. I know of no analytic solution valid on all scales at all times. To make progress, we will have to take some limits which reduce the full set of five equations to a more managable two or three. The cost is that these limits will be valid only for certain scales at certain times. Patching these analytic solutions together to obtain a reasonable transfer function is as much art as science.

As a guide to this analytic work which will occupy us much of the rest of this chapter, consider Figure 7.5. The solid curve is the comoving horizon (conformal time), which increases with time, equal to about $30\,h^{-1}$ Mpc at the epoch of

[1] This is a fairly good approximation since in most models, the baryon density is much smaller than the dark matter density. We will explore the effects of baryons in Section 7.6.

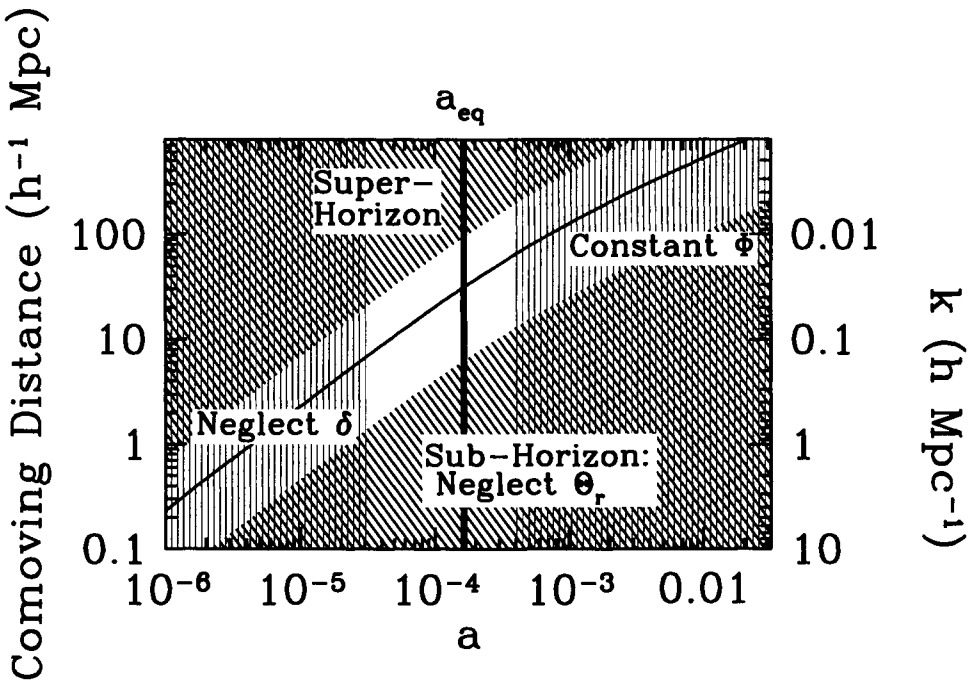

Figure 7.5. Physics of the transfer function. Hatched regions show where analytic expressions exist. The gaps in the center show that no analytic solutions exist to capture the full evolution of intermediate scale modes. The curve monotonically increasing from bottom left to top right is the comoving horizon.

equality.[2] A given comoving scale remains constant with time. Take for example, a comoving distance of $10\,h^{-1}$ Mpc, corresponding to wavenumber $k = 0.1\,h$ Mpc^{-1}. At early times ($a < 10^{-5}$) this distance is larger than the horizon, so $k\eta \ll 1$. We can then drop all terms proportional to k in the evolution equations. In Section 7.2.1, we will derive an exact solution for the potential in this super-horizon limit. Unfortunately, Figure 7.5 indicates that, for the mode in question, this super-horizon solution is valid only until $a \simeq 10^{-5}$. At much later times ($a > 10^{-3}$) the mode is well within the horizon and the radiation perturbations have become irrelevant (since the universe is matter dominated). We will see in Section 7.3.2 that, under these conditions, another analytic solution can be found. The difficulty is matching the super-horizon solution to the sub-horizon solution.

The problem of matching the super-horizon solution to the sub-horizon solution can be solved for very large scale ($k < 0.01\,h$ Mpc^{-1}) and very small scale ($k > 0.5\,h$ Mpc^{-1}) modes. In the large-scale case, we will see in Section 7.2.2 that once the universe becomes matter dominated, Φ = constant is a solution to the evolution

[2]This is model dependent; the plot shows sCDM, with $h = 0.5$.

equations even as the mode crosses the horizon. This fact serves as a bridge between the super- and sub-horizon solutions, both of which have constant Φ in the matter-dominated regime. In the small-scale case, we can neglect matter perturbations as the mode crosses the horizon, since these modes cross the horizon when the universe is deep in the radiation era. Then, once the mode is sufficiently within the horizon, radiation perturbations decay away, and we can match on to the sub-horizon, no-radiation perturbation solution of Section 7.3.2.

With analytic expressions on both large and small scales, we can obtain a good fit to the transfer function by splining the two solutions together. We will see in Section 7.4 that this works, primarily because the transfer function is so smooth, monotonically decreasing from unity on large scales.

7.2 LARGE SCALES

On very large scales, we can get analytic solutions for the potential first through the matter–radiation transition and then through horizon crossing. We start with the super-horizon solution valid through the matter–radiation transition. The results of Section 7.2.1 will be that the potential drops by a factor of 9/10 as the universe goes from radiation to matter domination.

7.2.1 Super-horizon Solution

For modes that are far outside the horizon, $k\eta \ll 1$ and we can drop all terms in the evolution equations dependent on k. From Eqs. (7.11) and (7.13), we see that, in this limit, the velocities (v and $\Theta_{r,1}$) decouple from the evolution equations. This immediately reduces the number of equations to solve from five to three. For the third equation, we notice that Eq. (7.16) has terms inversely proportional to k. These will be difficult to deal with, so let us choose Eq. (7.15) instead. We are left with

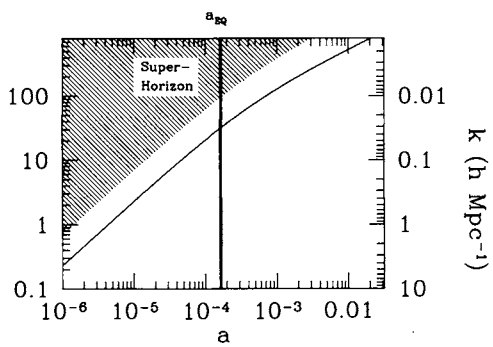

$$\dot{\Theta}_{r,0} = -\dot{\Phi} \tag{7.17}$$

$$\dot{\delta} = -3\dot{\Phi} \tag{7.18}$$

$$3\frac{\dot{a}}{a}\left(\dot{\Phi} + \frac{\dot{a}}{a}\Phi\right) = 4\pi G a^2 \left[\rho_{\rm dm}\delta + 4\rho_r\Theta_{r,0}\right]. \tag{7.19}$$

We can go a step further by realizing that the first two equations require $\delta - 3\Theta_{r,0}$ to be constant. Further, we know that this constant is zero (these are the initial

conditions). So let us use the dark matter equation (7.18) and the Einstein equation with $\Theta_{r,0}$ set to $\delta/3$. The Einstein equation is then

$$3\frac{\dot{a}}{a}\left(\dot{\Phi}+\frac{\dot{a}}{a}\Phi\right)=4\pi G a^2\rho_{\rm dm}\delta\left[1+\frac{4}{3y}\right]. \tag{7.20}$$

Here I have introduced

$$y\equiv\frac{a}{a_{\rm eq}}=\frac{\rho_{\rm dm}}{\rho_r} \tag{7.21}$$

which we will use as an evolution variable instead of η or a. Again I emphasize that we are ignoring baryons, so $a_{\rm eq}$ is determined solely by $\rho_{\rm dm}$; in the real world, the numerator in the last term in Eq. (7.21) would be $\rho_{\rm m}$, accounting for all matter including baryons.

Equations (7.18) and (7.20) are two first-order equations for the two variables δ and Φ. The stategy will be to turn these two first-order equations into one second-order equation and then solve. First, though, let us rewrite the equations in terms of the new variable y. The derivative with respect to y is related to that with respect to η via the Jacobian,

$$\begin{aligned}\frac{d}{d\eta}&=\frac{dy}{d\eta}\frac{d}{dy}\\&=aHy\frac{d}{dy},\end{aligned} \tag{7.22}$$

where the second line follows from the definition of y and the fact that $\dot{a}=a^2H$. In terms of y then, the Einstein equation becomes

$$\begin{aligned}y\Phi'+\Phi&=\frac{y}{2(y+1)}\delta\left[1+\frac{4}{3y}\right]\\&=\frac{3y+4}{6(y+1)}\delta\end{aligned} \tag{7.23}$$

where prime denotes derivatives with respect to y and the right side of the first line follows since $8\pi G\rho_{\rm dm}/3=(8\pi G\rho/3)y/(y+1)=H^2y/(y+1)$.

In general, to turn two first-order equations into one second-order equation, the trick is to differentiate one of them. Here, to simplify the algebra, we first rewrite Eq. (7.23) as an expression for δ; then differentiate with respect to y; and finally set δ' to $-3\Phi'$ thanks to the dark matter equation (7.18). This leads to

$$-3\Phi'=\frac{d}{dy}\left\{\frac{6(y+1)}{3y+4}\left[y\Phi'+\Phi\right]\right\}. \tag{7.24}$$

Carrying out the derivative is tedious but straightforward. We are left with

$$\Phi''+\frac{21y^2+54y+32}{2y(y+1)(3y+4)}\Phi'+\frac{\Phi}{y(y+1)(3y+4)}=0. \tag{7.25}$$

Remarkably, Kodama and Sasaki (1984) found an analytic solution to Eq. (7.25). They introduced a new variable

$$u \equiv \frac{y^3}{\sqrt{1+y}}\Phi. \tag{7.26}$$

In terms of this variable, you will show (Exercise 4) that Eq. (7.25) becomes

$$u'' + u'\left[\frac{-2}{y} + \frac{3/2}{1+y} - \frac{3}{3y+4}\right] = 0. \tag{7.27}$$

That is, there is no term proportional to u. Instead of a second-order equation for Φ, then, we have a first-order equation for u'. Fortunately, this first-order equation is integrable. Starting from

$$\frac{du'}{u'} = dy\left[\frac{2}{y} - \frac{3/2}{1+y} + \frac{3}{3y+4}\right], \tag{7.28}$$

we can integrate to get

$$\ln(u') = \text{constant} + 2\ln(y) - (3/2)\ln(1+y) + \ln(3y+4). \tag{7.29}$$

Then exponentiating gives

$$u' = A\frac{y^2(3y+4)}{(1+y)^{3/2}} \tag{7.30}$$

where A is a constant to be determined.

We are one integral away from an analytic expression for the gravitational potential. Remembering the definition of u (Eq. (7.26)), we can integrate Eq. (7.30) to obtain

$$\frac{y^3}{\sqrt{1+y}}\Phi = A\int_0^y dy' \frac{y'^2(3y'+4)}{(1+y')^{3/2}}. \tag{7.31}$$

Note that there should be another constant, $u(0)$, here. However, since $y^3\Phi \to 0$ early on, this constant is vanishes. By similar logic, we can determine the constant A even before performing the integral. For small y, the integrand becomes $4y'^2$, so for small y, Eq. (7.31) becomes $\Phi = 4A/3$. Therefore, $A = 3\Phi(0)/4$. The integral can be done analytically (Exercise 4 again) leaving

$$\Phi = \frac{\Phi(0)}{10}\frac{1}{y^3}\left[16\sqrt{1+y} + 9y^3 + 2y^2 - 8y - 16\right]. \tag{7.32}$$

Equation (7.32) is our final expression for the potential on super-horizon scales. Although it is not obvious, at small y this expression sets $\Phi = \Phi(0)$, a constant. This must be so, since we chose the two constants of integration with precisely this condition. At large y, once the universe has become matter-dominated, the y^3 term in the brackets dominates, so $\Phi \to (9/10)\Phi(0)$. This is precisely the result we were after: the potential on even the largest scales drops by 10% as the universe passes through the epoch of equality.

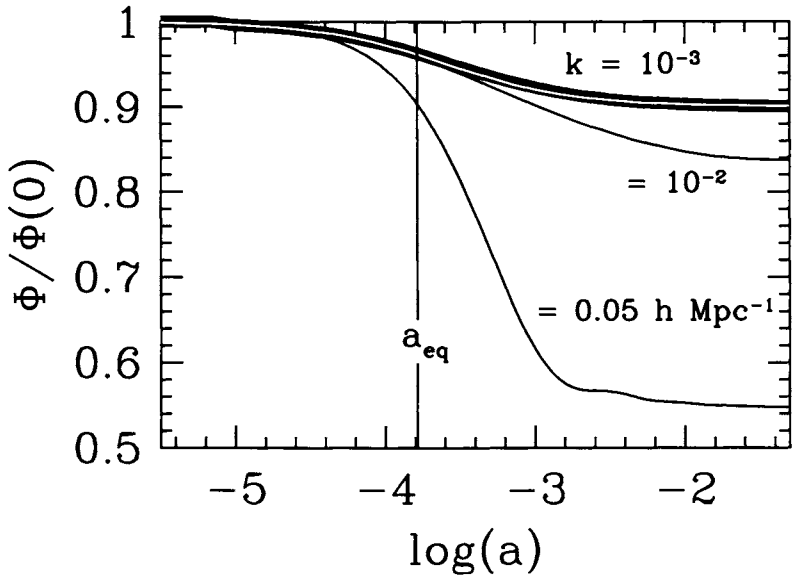

Figure 7.6. Super-horizon evolution of the potential in a CDM model with no baryons, $h = 0.5$ and $\Omega_m = 1$. Thick solid line shows the analytic result of Eq. (7.32), valid only on large scales. White curve within is for the mode $k = 0.001\,h$ Mpc^{-1}. Two other smaller scale modes are shown.

Let us compare this analytic result, valid only when modes are super-horizon, with the numerical results. Figure 7.6 shows that the solution works perfectly on the largest scales and even tolerably well (better than 10%) for scales as small as $k = 0.01\,h$ Mpc^{-1}. This is slightly better than we had anticipated from a crude estimate of where the super-horizon solution is valid (Figure 7.5) and will be important for us later on when spline together the large and small scales solutions. A feature of the analytic solution which may be surprising to you is that, although it is true that the (large scale) potentials are constant in both the matter and radiation epochs, the transition between the pure matter and pure radiation eras is quite long. For example, and this is an important example for the purposes of the CMB as we will see in the next chapter, the potentials, even for the largest scale modes, are still decaying as late as $a \simeq 10^{-3}$, significantly after $a_{\rm eq}$. In models with less matter, $a_{\rm eq}$ is pushed even closer to 10^{-3} so the decay of the potentials becomes even more apparent at the time of recombination.

7.2.2 Through Horizon Crossing

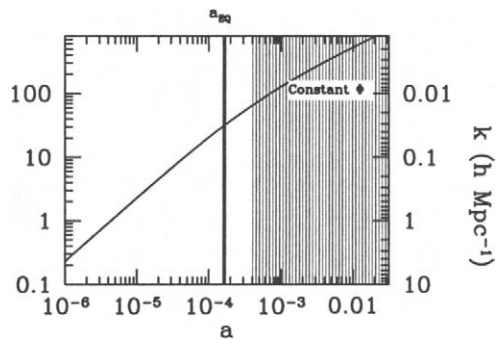

One interesting feature of Figure 7.6 which you should take note of is that large-scale potential (the numerical solution) becomes constant at very late times ($a \gtrsim 10^{-2}$). For $k = 10^{-3}\,h$ Mpc^{-1}, the mode enters the horizon at $\eta \sim k^{-1} = 1000\,h^{-1}$ Mpc which corresponds to $a \sim 0.03$ in the flat, matter-dominated universe depicted in Figure 7.6. The potential remains constant as the mode crosses the horizon. This result is valid as long as the universe is matter dominated. We now set out to prove it.

We are interested then in our set of five equations in the limit that radiation is not important. The potential depends only on the matter inhomogeneities, so we can neglect the two radiation equations, (7.11) and (7.12). In addition to the two matter equations, we now keep the second of Einstein's equations (7.16). This is an algebraic equation, meaning that we could in principle eliminate Φ in the two matter equations and be left with a system of two first-order differential equations. These two first-order equations in general have two solutions. Instead of solving them directly, though, we can cheat using our knowledge of the initial conditions. Here is the idea: we just learned that, deep in the matter epoch, super-horizon potentials are constant. Therefore, the initial conditions for our problem are that the potential is constant ($\dot{\Phi} = 0$). If we can show that constant Φ is one of the two general solutions to the set of matter-dominated equations, then we don't care what the other solution is. For, the initial conditions ensure that the constant Φ solution will be *the* solution.

We want to see, then, if the set of equations

$$\dot{\delta} + ikv = 0 \tag{7.33}$$

$$\dot{v} + aHv = ik\Phi \tag{7.34}$$

$$k^2\Phi = \frac{3}{2}a^2H^2\left[\delta + \frac{3aHiv}{k}\right] \tag{7.35}$$

admits a solution with Φ a constant in time. We can use the algebraic equation (7.35) to eliminate δ from the other two equations. In the matter dominated era, $H \propto a^{-3/2}$, so $d(aH)/d\eta = -a^2H^2/2$. Replacing δ in Eq. (7.33) with Φ and v therefore leads to

$$\frac{2k^2\dot{\Phi}}{3a^2H^2} + \frac{2k^2\Phi}{3aH} - \frac{3aHi\dot{v}}{k} + \frac{3a^2H^2iv}{2k} + ikv = 0. \tag{7.36}$$

We now have two first-order equations for Φ and v. The strategy is to turn these two equations into one second-order equation for Φ. First eliminate $\dot{v}$ from Eq. (7.36) by using the velocity equation. This leaves

$$\frac{2k^2\dot{\Phi}}{3a^2H^2} + \left[\frac{iv}{k} + \frac{2\Phi}{3aH}\right]\left(\frac{9a^2H^2}{2} + k^2\right) = 0. \tag{7.37}$$

If the second-order equation is of the form $\alpha\ddot{\Phi} + \beta\dot{\Phi} = 0$, that is, if it has no terms proportional to Φ, then $\Phi =$ constant is a solution to the equations. So we differentiate Eq. (7.37) with respect to η but consider only the terms proportional to Φ, dropping all terms proportional to derivatives of Φ. Using the fact that $(d/d\eta)(aH)^{-1} = 1/2$, we see that the remaining terms are

$$\left[\frac{i\dot{v}}{k} + \frac{\Phi}{3}\right]\left(\frac{9a^2H^2}{2} + k^2\right) + \left[\frac{iv}{k} + \frac{2\Phi}{3aH}\right]\frac{d}{d\eta}\frac{9a^2H^2}{2}$$

$$= -\left[\frac{iaHv}{k} + \frac{2\Phi}{3}\right](9a^2H^2 + k^2) \tag{7.38}$$

where I have eliminated $\dot{v}$ by using the velocity equation again. But Eq. (7.37) tells us that the term in square brackets on the right here is proportional to $\dot{\Phi}$. So there are no terms in the second-order equation proportional to Φ. Constant potentials are therefore a solution in the matter-dominated era. Since the initial conditions pick out this mode, constant potential is *the* solution in the matter-dominated era.

Potentials remain constant as long as the universe is matter dominated. At much later times ($a > 1/10$), it is conceivable that the universe becomes dominated by some other form of energy — dark energy for example — or, less likely, by curvature. If so, then the potentials will decay. This decay is described by the growth function, though (Section 7.5), and does not affect the transfer function. The main result of this section is that the transfer function as defined in Eq. (7.3) is very close to unity on all scales that enter the horizon after the universe becomes matter dominated. That is, it is unity for all $k \ll a_{\rm eq}H(a_{\rm eq})$, the inverse comoving Hubble radius at equality. You will show in Exercise 5 that the relevant scale is

$$k_{\rm eq} = 0.073{\rm Mpc}^{-1}\Omega_m h^2. \tag{7.39}$$

In the limit in which we are working, where baryons and anisotropic stresses are neglected, the transfer function depends only on $k/k_{\rm eq}$. To get a feel for when the large-scale approximations of this section are valid, look back at Figure 7.6, plotted for the standard CDM model with $\Omega_m = 1$ and $h = 0.5$. The transfer function for the curve labeled 10^{-2} is 7% lower (0.84/0.9) than unity. For that mode, $k/k_{\rm eq} = 0.01/(0.073h) = 0.27$. So if we are interested in 10% accuracy in the transfer function, then we can use the large-scale approximation for $k \lesssim k_{\rm eq}/3$.

7.3 SMALL SCALES

We were able to solve for the evolution of large-scale perturbations in the previous section because the modes crossed the horizon well *after* the epoch of equality. Therefore, the problem neatly divided into (i) super-horizon modes passing through the epoch of equality and then (ii) modes in the matter-dominated era which cross

the horizon. The converse is true for the small-scale modes considered in this section. They cross the horizon when the universe is deep in the radiation era. So the problem divides neatly into (i) modes in the radiation era crossing the horizon and then (ii) sub-horizon modes passing through the epoch of equality. Step (i) we treat in Section 7.3.1, step (ii) in Section 7.3.2. Notice that we are unable to treat analytically modes which enter the horizon around the epoch of equality.

7.3.1 Horizon Crossing

When the universe is radiation dominated, the potential is determined by perturbations to the radiation. The dark matter perturbations—the ones we are interested in in this chapter—are influenced by the potential, but do not themselves influence the potential. So the situation is as depicted in Figure 7.7. To solve for matter perturbations in this epoch, therefore, is a two-step problem. First, we must solve the coupled equations for $\Theta_{r,0}, \Theta_{r,1}$, and Φ. Then we solve the equation for matter evolution using the potential as an external driving force.

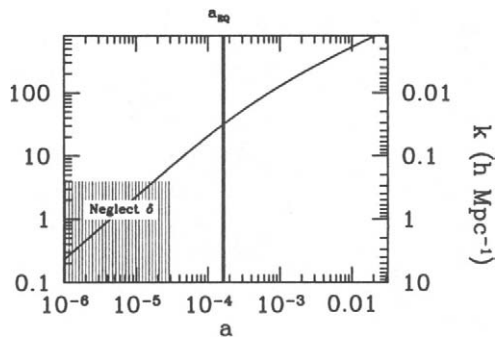

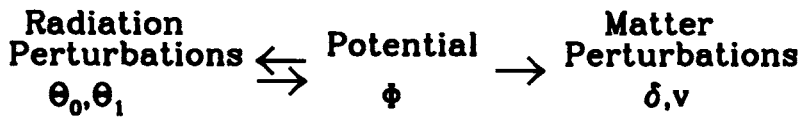

Figure 7.7. Coupling of perturbations in the radiation era. Radiation perturbations and the gravitational potential affect each other. Matter perturbations do not affect the potential but are driven by it.

To solve for the potential in the radiation dominated era, we choose Eq. (7.16). Dropping the matter source terms, we have

$$\Phi = \frac{6a^2H^2}{k^2}\left[\Theta_{r,0} + \frac{3aH}{k}\Theta_{r,1}\right] \tag{7.40}$$

since $H^2 = 8\pi G\rho_r/3$ in the radiation era. Also in the radiation era, $aH = 1/\eta$. Armed with this fact, we can use Einstein's equation (7.40) to eliminate $\Theta_{r,0}$ from the two radiation equations, (7.11) and (7.12). These become

$$-\frac{3}{k\eta}\dot{\Theta}_{r,1} + k\Theta_{r,1}\left[1 + \frac{3}{k^2\eta^2}\right] = -\dot{\Phi}\left[1 + \frac{k^2\eta^2}{6}\right] - \Phi\frac{k^2\eta}{3} \tag{7.41}$$

$$\dot{\Theta}_{r,1} + \frac{1}{\eta}\Theta_{r,1} = \frac{-k}{3}\Phi\left[1 - \frac{k^2\eta^2}{6}\right] \tag{7.42}$$

We can turn these two first order-equations for Φ and $\Theta_{r,1}$ into one second-order equation for the potential. Use Eq. (7.42) to eliminate $\dot{\Theta}_{r,1}$ from the first equation, which then becomes

$$\dot{\Phi} + \frac{1}{\eta}\Phi = \frac{-6}{k\eta^2}\Theta_{r,1}. \tag{7.43}$$

We now have an expression for $\Theta_{r,1}$ solely in terms of the potential and its first derivative. To arrive at a second-order equation for Φ, we differentiate. When we do, we will encounter terms proportional to $\Theta_{r,1}$ and its derivative. Each of these can be eliminated with Eq. (7.42) and Eq. (7.43). The resulting second-order equation is

$$\ddot{\Phi} + \frac{4}{\eta}\dot{\Phi} + \frac{k^2}{3}\Phi = 0. \tag{7.44}$$

To determine the behavior of the potential in the radiation-dominated era, we must solve Eq. (7.44) subject to the initial conditions that Φ is constant. It can be solved analytically by defining $u \equiv \Phi\eta$. Then Eq. (7.44) becomes

$$\ddot{u} + \frac{2}{\eta}\dot{u} + \left(\frac{k^2}{3} - \frac{2}{\eta^2}\right)u = 0. \tag{7.45}$$

This is the spherical Bessel equation of order 1 (see Eq. (C.13)) with solutions $j_1(k\eta/\sqrt{3})$—the spherical Bessel function—and $n_1(k\eta/\sqrt{3})$—the spherical Neumann function. The latter blows up as η gets very small, so we discard it on the basis of the initial conditions. The spherical Bessel function of order 1 can be expressed in terms of trigonometric functions (Eq. (C.14)), so

$$\Phi = 3\Phi_{\rm p}\left(\frac{\sin(k\eta/\sqrt{3}) - (k\eta/\sqrt{3})\cos(k\eta/\sqrt{3})}{(k\eta/\sqrt{3})^3}\right) \tag{7.46}$$

where $\Phi_{\rm p}$ is the primordial value of Φ. The factor of 3 in front here arises because the $\eta \to 0$ limit of the expression in parentheses is $1/3$.

Equation (7.46) tells us that, as soon as a mode enters the horizon during the radiation-dominated era, its potential starts to decay. After decaying, the potential oscillates, as depicted in Figure 7.8. Qualitatively, we could have anticipated as much. From the qualitative discussion surrounding Eq. (7.1), we expected that when the pressure is large, as it is when radiation dominates, perturbations will oscillate in time. If perturbations to the dominant component (here radiation) do not grow, then the potential in an expanding universe will begin to decay simply due to the dilution of the zero-order density. This is evident in Eq. (7.40) which (neglecting the dipole well within the horizon) says that $\Phi \sim \Theta_0/\eta^2$. Since Θ_0 oscillates with fixed amplitude, the potential also ocillates, but with an amplitude decreasing as η^{-2}. Indeed, this is precisely the large $k\eta$ limit of Eq. (7.46). The decay and oscillation of the potential is shown in Figure 7.8, with both the analytic

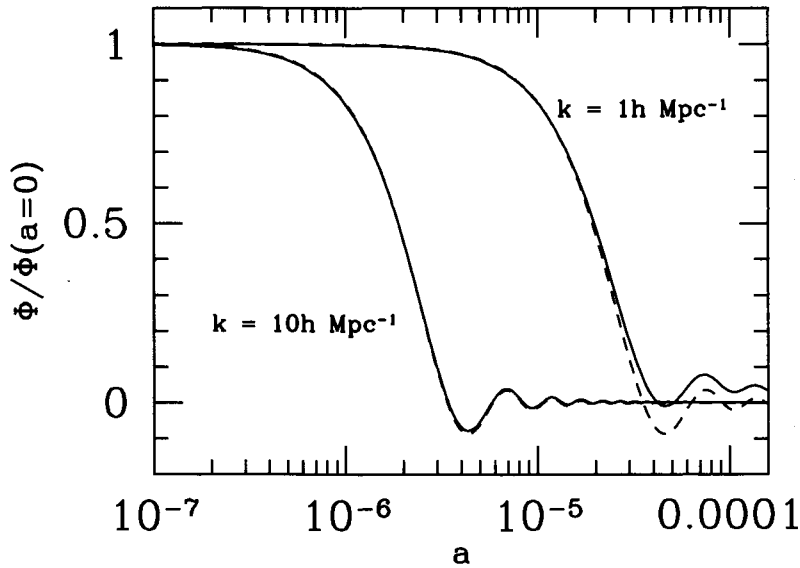

Figure 7.8. Evolution of the potential in the radiation-dominated era. For two small scale modes which enter the horizon well before equality, the exact (solid curve) solution is shown along with the approximate analytic solution (dashed curve) of Eq. (7.46).

expression of Eq. (7.46) and the numerical solution including matter perturbations. Note that the approximate description — in which the effect of matter on the potential is neglected — is valid only deep in the radiation era. The analytic solution for the $k = 1\,h$ Mpc^{-1} mode already begins to depart from the exact solution at $a \simeq 3 \times 10^{-5}$, well before equality (here, in the sCDM model I have taken for illustrative purposes, at $a \simeq 2 \times 10^{-4}$).

Armed with knowledge of the potential in the radiation dominated era, we can now determine the evolution of the matter perturbations, the second half of Figure 7.7. To do this, we turn the two matter evolution equations — (7.13) and (7.14) — into one second-order equation with the potentials serving as an external source. Differentiate Eq. (7.13) and use Eq. (7.14) to eliminate $\dot{v}$:

$$\ddot{\delta} + ik\left(-\frac{\dot{a}}{a}v + ik\Phi\right) = -3\ddot{\Phi}. \tag{7.47}$$

Now we can use Eq. (7.13) to eliminate v, leading to

$$\ddot{\delta} + \frac{1}{\eta}\dot{\delta} = S(k,\eta) \tag{7.48}$$

where the source term is

$$S(k,\eta) = -3\ddot{\Phi} + k^2\Phi - \frac{3}{\eta}\dot{\Phi}. \tag{7.49}$$

The two solutions to the homogeneous equation ($S = 0$) associated with Eq. (7.48) are δ = constant and $\delta = \ln(a)$ (or, equivalently in the radiation-dominated era, $\ln[\eta]$). In general, the solution to a second-order equation is a linear combination of the two homogeneous solutions and a particular solution. In the absence of a revelation about the particular solution, one can construct it from scratch from the two homogeneous solutions (call them s_1 and s_2) and the source terms. It is the integral of the source term weighted by the Green's function $[s_1(\eta)s_2(\eta') - s_1(\eta')s_2(\eta)]/[\dot{s}_1(\eta')s_2(\eta') - s_1(\eta')\dot{s}_2(\eta')]$. So here, we have

$$\delta(k,\eta) = C_1 + C_2 \ln(\eta) - \int_0^\eta d\eta' S(k,\eta')\eta' \left(\ln[k\eta'] - \ln[k\eta]\right). \tag{7.50}$$

At very early times the integral is small, so our initial conditions (δ constant) dictate that the coefficient of $\ln(\eta)$, C_2, vanishes and $C_1 = \delta(k, \eta = 0) = 3\Phi_\mathrm{p}/2$. Now let us consider the integral in Eq. (7.50). The source function decays to zero along with the potential as the mode enters the horizon. Thus, the dominant contribution to the integral comes from the epochs during which $k\eta$ is of order 1. The integral over $S(\eta')\ln(k\eta')$ therefore will just asymptote to some constant, while the integral over $S(\eta')\ln(k\eta)$ will lead to a term proportional to $\ln(k\eta)$ with the constant of proportionality being just that, a constant. Thus, we expect that after the mode has entered into the horizon,

$$\delta(k,\eta) = A\Phi_\mathrm{p} \ln(Bk\eta), \tag{7.51}$$

i.e., a constant ($A\Phi_\mathrm{p}\ln[B]$) plus a logarithmic growing mode ($A\Phi_\mathrm{p}\ln[k\eta]$).

We can determine the constants A and B in Eq. (7.51) by referring to the relevant parts of Eq. (7.50). The constant term, $A\Phi_\mathrm{p}\ln(B)$, is equal to C_1 plus the integral over $\ln(\eta')$, or

$$A\Phi_\mathrm{p}\ln(B) = \frac{3}{2}\Phi_\mathrm{p} - \int_0^\infty d\eta' S(k,\eta')\eta' \ln(k\eta'), \tag{7.52}$$

while the coefficient of the $\ln(k\eta)$ term is set by the remaining integral

$$A\Phi_\mathrm{p} = \int_0^\infty d\eta' S(k,\eta')\eta'. \tag{7.53}$$

Note that in both integrals here, I have set the upper limit to infinity in accord with our expectation that the integrals asymptote to some constant value at large η. Using the expression for the source term, Eq. (7.49), and our analytic approximations to the potential, Eq. (7.46), we can evaluate the integrals here and determine A and B. I find $A = 9.0$ and $B = 0.62$. Hu and Sugiyama (1996), who introduced this method for following the dark matter evolution at early times, found that integrating the exact potentials (instead of the approximate ones of Eq. (7.46)) leads to slightly different values, $A = 9.6$ and $B = 0.44$.

Figure 7.9 shows the exact solution for δ in the radiation era along with the approximation of Eq. (7.51). Setting aside the details for a moment, we see that

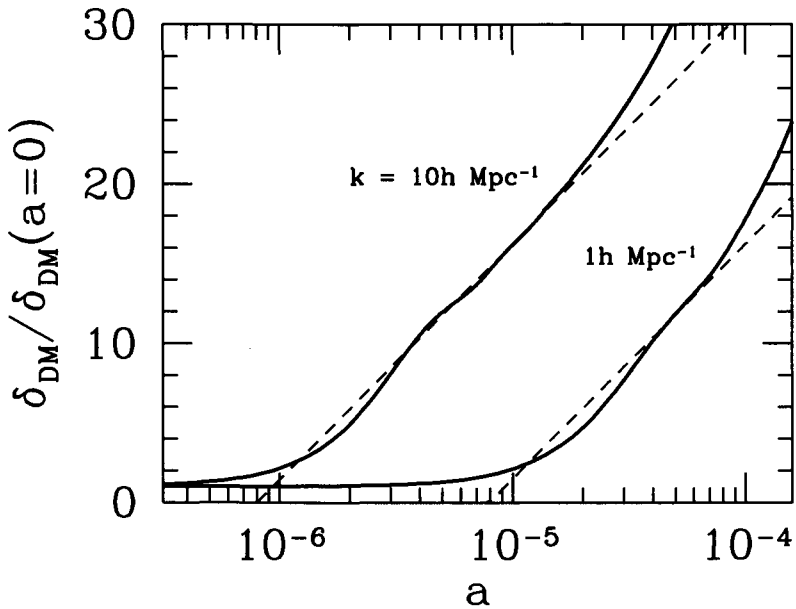

Figure 7.9. Matter perturbations in the radiation-dominated era. The two scales shown here both enter the horizon in the radiation era and lock onto the logarithmically growing mode after some oscillations. Heavy solid curves are the exact solutions, light dashed curves the logarithmic mode of Eq. (7.51). The perturbations have been artificially normalized by their values at early times: inflation actually predicts a larger initial amplitude (by a factor of $10^{3/2}$) for the larger scale mode.

matter perturbations do indeed grow even during the radiation era. The growth is not as prominent as during the matter era (when the constant potentials derived in Section 7.2 imply $\delta \propto a$) due to the pressure of the radiation, but it still exists. For both scales shown in Figure 7.9 the perturbations do indeed settle into the logarithmic growing mode once they enter the horizon. As the universe gets closer to matter domination, though, the pressure of the radiation becomes less important, and the perturbations begin to grow faster. Indeed, you might be worried that our approximation for the $k = 1\,h$ Mpc^{-1} mode is not very useful. Fortunately, we will be using these solutions only to set the initial conditions for growth in the sub-horizon epoch (next subsection), so the approximation need be valid only for a very limited range of times. As long as we choose the matching epoch appropriately, the logarithmic approximation will be extremely good.

7.3.2 Sub-horizon Evolution

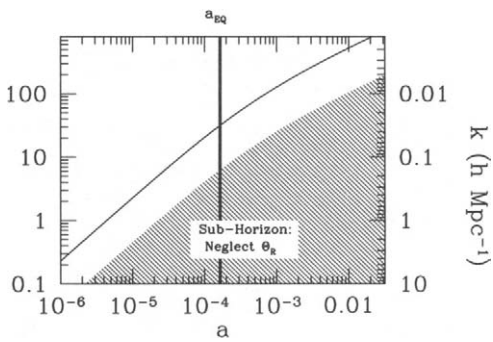

We saw in the last subsection that radiation pressure causes the gravitational potentials to decay as modes enter the horizon during the radiation era. Although I did not focus on the radiation perturbations themselves (we will do this in the next chapter), you might expect that the pressure suppresses any growth in $\Theta_{r,0}$. This is correct, and it is in sharp contrast to the matter perturbations which, we just saw, grow logarithmically. Although initially the potential is determined by the radiation (since the universe is radiation dominated), eventually the growth in the matter perturbations more than offsets the fact that there is more radiation than matter. That is, eventually $\rho_{\rm dm}\delta$ becomes larger than $\rho_r\Theta_{r,0}$ even if $\rho_{\rm dm}$ is smaller than ρ_r. Once this happens, the gravitational potential and the dark matter perturbations evolve together and do not care what happens to the radiation. In this subsection, we want to solve the set of equations governing the matter perturbations and the potential and then match on to the logarithmic solution (7.51) set up during the epoch in which the potential decays.

Once again our starting point is the set of equations governing dark matter evolution, (7.13) and (7.14), and the algebraic equation for the gravitational potential (7.16). And, once again, we want to reduce this set of three equations (two of which are first-order differential equations) to one second-order equation. We will want to follow the sub-horizon dark matter perturbations through the epoch of equality, so it proves convenient again to use y (Eq. (7.21)) — the ratio of the scale factor to its value at equality — as the evolution variable. In terms of y, the three equations become

$$\delta' + \frac{ikv}{aHy} = -3\Phi' \tag{7.54}$$

$$v' + \frac{v}{y} = \frac{ik\Phi}{aHy} \tag{7.55}$$

$$k^2\Phi = \frac{3y}{2(y+1)}a^2H^2\delta. \tag{7.56}$$

Several comments are in order about this version of our fundamental equations. First, notice that the time derivatives in the first two equations have been replaced by derivatives with respect to y (indicated by primes), and this transformation leads to the factors of $\dot{y} = aHy$ in the denominators of the unprimed terms. Second, the gravitational potential is now expressed solely in terms of δ: there is no dependence on radiation perturbations because of our arguments above that these are subdominant, and there is no aHv/k dependence because the perturbations are well within the horizon and $aH/k \ll 1$. Finally, the coefficient of the δ source term

is $4\pi G\rho_{\rm dm}a^2 \to (3/2)a^2H^2y/(y+1)$ since we are interested in times early enough that any curvature or dark energy is negligible.

We now go through the familiar routine of turning Eqs. (7.54) and (7.55) into a second-order equation for δ: differentiate the first of these to get

$$\delta'' - \frac{ik(2+3y)v}{2aHy^2(1+y)} = -3\Phi'' + \frac{k^2\Phi}{a^2H^2y^2} \tag{7.57}$$

where v' has been eliminated using the velocity equation. Also I have used the fact that $d(1/aHy)/dy = -(1+y)^{-1}(2aHy)^{-1}$. The first term on the right is much smaller than the second, since the latter is multiplied by $(k/aH)^2$, and we are focusing on sub-horizon modes. Using Eq. (7.56), we recognize this second term as $3\delta/[2y(y+1)]$. We can rewrite the velocity on the left using Eq. (7.54) but neglecting the potential which on sub-horizon scales is much smaller than δ. Thus, the combination $ikv/(aHy)$ can be simply replaced by $-\delta'$ leaving

$$\delta'' + \frac{2+3y}{2y(y+1)}\delta' - \frac{3}{2y(y+1)}\delta = 0. \tag{7.58}$$

This is the *Meszaros equation* governing the evolution of sub-horizon cold, dark matter perturbations once radiation perturbations have become negligible.

To understand the growth of dark matter perturbations, we need to obtain the two independent solutions to the Meszaros equations and then match on to the logarithmic mode established in the previous subsection. To solve this differential equation, we can use our knowledge of the solution deep in the matter era. We know that sub-horizon perturbations in the matter era grow with the scale factor, so one of the solutions to Eq. (7.58) is a polynomial in y of order 1. Therefore, for one mode at least, δ'' vanishes. Therefore, the equation governing this first mode, the growing mode,[3] is $D_1'/D_1 = 3/(2+3y)$, the solution to which is

$$D_1(y) = y + 2/3. \tag{7.59}$$

To find the second solution, notice that the Meszaros equation tells us that $u \equiv \delta/D_1$ satisfies

$$(1+3y/2)u'' + \frac{u'}{y(y+1)}[(21/4)y^2 + 3y + 1] = 0. \tag{7.60}$$

Since there is no term proportional to u, Eq. (7.60) is actually a first-order equation[4] for u'. We can therefore integrate to obtain a solution for u' and then integrate again to get the second Meszaros solution. The first integral gives

[3] D_1 is the *growth function* mentioned in Section 7.1. Note though that in this section we are assuming that only matter, and not curvature or dark energy, dominates the landscape. Therefore, our expression for the growth function will be valid only when $a \lesssim 0.1$. For the generalization to later times, see Section 7.5.

[4] Indeed this is a general trick for obtaining the second solution to a differential equation once the first is known. We will use it again later on to obtain the growth factor.

$$u' \propto (y + 2/3)^{-2} y^{-1} (y + 1)^{-1/2}. \tag{7.61}$$

Integrating again leads to the second Meszaros solution

$$D_2(y) = D_1(y) \ln \left[\frac{\sqrt{1+y} + 1}{\sqrt{1+y} - 1} \right] - 2\sqrt{1+y}. \tag{7.62}$$

At late times ($y \gg 1$), the growing solution D_1 scales as y while the decaying mode D_2 falls off as $y^{-3/2}$.

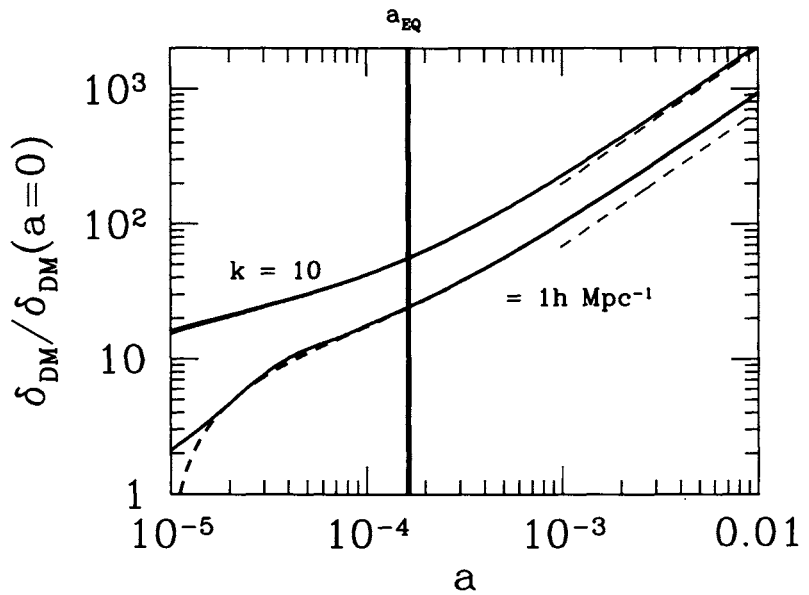

Figure 7.10. Evolution of small-scale, sub-horizon, dark matter perturbations. Solid curves are exact solutions; dashed curves (almost imperceptible because the goodness of fit in the $10\,h$ Mpc^{-1} case) the Meszaros solution with coefficients given by the matching condition, Eq. (7.64). The dashed straight lines at $a > 10^{-3}$ are the asymptotic solution of Eq. (7.67).

The general solution to the Meszaros equation is therefore

$$\delta(k, y) = C_1 D_1(y) + C_2 D_2(y) \qquad y \gg y_H \tag{7.63}$$

where y_H is the scale factor when the mode enters the horizon divided by the scale factor at equality (Exercise 6). To determine the constants C_1 and C_2 we can match on to the logarithmic solution of Eq. (7.51). That solution is valid within the horizon but before equality: $y_H \ll y \ll 1$. So we can hope to arrive at a reasonable approximation for the evolution of dark matter perturbations only for those modes that enter the horizon before equality. For those modes, we match the two solutions and their first derivatives

$$A\Phi_{\rm p} \ln(B y_m / y_H) = C_1 D_1(y_m) + C_2 D_2(y_m)$$

$$\frac{A\Phi_{\rm p}}{y_m} = C_1 D_1'(y_m) + C_2 D_2'(y_m) \tag{7.64}$$

where the matching epoch y_m must satisfy $y_H \ll y_m \ll 1$. Note that I have replaced the argument of the log in Eq. (7.51) — $k\eta$ — with y/y_H, valid as long as the matching epoch is deep in the radiation era. Figure 7.10 shows the evolution of two modes along with the analytic solutions to the Meszaros equation with coefficients set by the matching conditions laid out in Eq. (7.64). Not suprisingly, for larger scale modes than the ones shown the approximation breaks down.

7.4 NUMERICAL RESULTS AND FITS

In Section 7.2 and Section 7.3, we derived analytic solutions following the dark matter perturbations deep into the matter era. Here, we assimilate these results and spline them together to form the transfer function. Also, I will present a well-known fitting function for the transfer function.

First, we need to transform our expression ((7.63) along with Eqs. (7.64)) for the small-scale matter density into an expression for the transfer function. The transfer function is determined by the behavior of δ well after equality when the decaying mode has long since vanished. We can extract an even simpler form for δ in this $a \gg a_{\rm eq}$ limit. The key constant in that case is C_1, the coefficient of the growing mode. Multiplying the first matching condition in Eq. (7.64) by D_2' and the second by D_2 and then subtracting leads to

$$C_1 = \frac{D_2'(y_m) A \ln(B y_m/y_H) - D_2(y_m)(A/y_m)}{D_1(y_m)D_2'(y_m) - D_1'(y_m)D_2(y_m)}\Phi_{\rm p}. \tag{7.65}$$

The denominator $D_1 D_2' - D_1' D_2 = -(4/9) y_m^{-1}(y_m+1)^{-1/2}$, which is approximately equal to $-4/9y_m$ since $y_m \ll 1$. Similarly for small y_m, $D_2 \to (2/3)\ln(4/y) - 2$ and $D_2' \to -2/3y$. Therefore,

$$C_1 \to \frac{-9A\Phi_{\rm p}}{4}\left[\frac{-2}{3}\ln(B y_m/y_H) - (2/3)\ln(4/y_m) + 2\right], \tag{7.66}$$

which fortuitously does not depend on y_m. Therefore, at late times we have an approximate solution for the small-scale dark matter perturbations

$$\delta(\vec{k}, a) = \frac{3A\Phi_{\rm p}(\vec{k})}{2}\ln\left[\frac{4Be^{-3}a_{\rm eq}}{a_H}\right] D_1(a) \qquad a \gg a_{\rm eq}. \tag{7.67}$$

On very small scales, the argument of the log simplifies because $a_{\rm eq}/a_H = \sqrt{2}k/k_{\rm eq}$ (Exercise 6). To turn Eq. (7.67) into a transfer function, we need to remember how δ is related to $\Phi_{\rm p}$. Comparing Eq. (7.8) with Eq. (7.67) leads to an analytic expression for the transfer function on small scales:

$$T(k) = \frac{5A\Omega_m H_0^2}{2k^2 a_{\rm eq}}\ln\left[\frac{4Be^{-3}\sqrt{2}k}{k_{\rm eq}}\right] \qquad k \gg k_{\rm eq}. \tag{7.68}$$

Recall that the wavenumber entering the horizon at equality is defined as $k_{\rm eq} \equiv a_{\rm eq}H(a_{\rm eq}) = \sqrt{2}H_0 a_{\rm eq}^{-1/2}$, so the prefactor is also a function of $k/k_{\rm eq}$ only. Then, plugging in numbers leads to

$$T(k) = \frac{12k_{\rm eq}^2}{k^2} \ln\left[\frac{k}{8k_{\rm eq}}\right] \qquad k \gg k_{\rm eq}. \tag{7.69}$$

Figure 7.11 shows the power spectrum for a standard CDM model ($n = 1$; $h = 0.5$; but no baryons) matching the large-scale transfer function ($T = 1$) with the small-scale transfer function of Eq. (7.69). Also shown is the exact solution

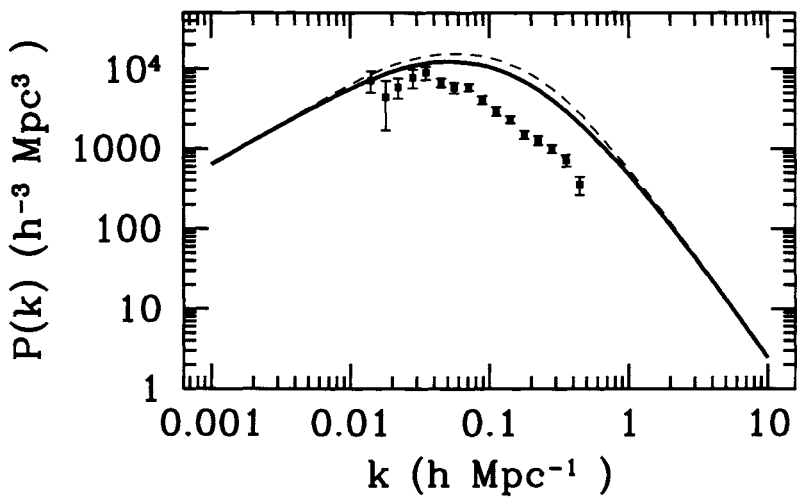

Figure 7.11. The power spectrum in a standard CDM model with a Harrison–Zel'dovich–Peebles spectrum. The thick solid curve uses the BBKS transfer function; the dashed curve interpolates between the analytic transfer function on large scales (equal to 1) and small scales (Eq. (7.68)). The data points are a compilation (and interpretation) by Peacock and Dodds (1994).

(again in the no-baryon limit), or equivalently, the fitting form of Bardeen, Bond, Kaiser, and Szalay (1986, BBKS),

$$T(x \equiv k/k_{\rm eq}) = \frac{\ln[1+0.171x]}{(0.171x)} \left[1 + 0.284x + (1.18x)^2 + (0.399x)^3 + (0.490x)^4\right]^{-0.25}. \tag{7.70}$$

Note that the BBKS form agrees very well with the analytic solution on small scales; i.e., both aymptote to $\ln(k)/k^2$ with the same coefficients. Since wavenumbers are measured in units of h Mpc^{-1}, the ratio $k/k_{\rm eq}$ depends on $\Omega_m h$. So defining $\Gamma \equiv \Omega_m h$, the BBKS transfer function can also be written as

$$T\left(q \equiv k/\Gamma h\,\mathrm{Mpc}^{-1}\right) = \frac{\ln[1+2.34q]}{(2.34q)}\left[1+3.89q+(16.2q)^2+(5.47q)^3+(6.71q)^4\right]^{-0.25}. \tag{7.71}$$

Several final comments are in order. First, our analytic work has enabled us to understand the origin of the asymptotic, small-scale behavior of the power spectrum. Had there been no logarithmic growth in the radiation era, the modes which entered very early on would have experienced no growth from horizon entry until the epoch of equality. Their amplitude relative to large-scale modes would then have been suppressed by a factor of order $(k_{\rm eq}/k)^2$. The logarithmic growing mode in the radiation era somewhat ameliorates this suppression. Second, although our analytic expression and its BBKS counterpart are good approximations, it is important to be aware of some small effects which affect the transfer function in the real world. We have assumed no anisotropic stresses ($\Phi = -\Psi$). Dropping this assumption changes the factor of 9/10 by which the potential drops for large-scale modes to 0.86, resulting in a corresponding rise in the small-scale transfer function. Including a realistic amount of baryons leads to even more severe small-scale changes. We will address these in Section 7.6. Third, all of our work in this section has been on the transfer function, i.e., on the evolution of perturbations early on when the only components of the universe were matter and radiation. At very late times, the growth function depends on other hypothetical components, the most likely of which is dark energy. Finally, the theoretical power spectrum in Figure 7.11 has been normalized by fixing δ_H in Eq. (7.9) using the observations of CMB anisotropies on large scales (more on this in Chapter 8). We see that (i) the large-scale normalization is roughly correct and that (ii) the shape of the standard CDM power spectrum is wrong. The sCDM power spectrum turns over on relatively small scales, in distinct disagreement with the data. The universe as we observe it appears to have a smaller $k_{\rm eq}$ than sCDM. This observation motivates consideration of variations of sCDM; we will consider these in Section 7.6.

7.5 GROWTH FUNCTION

At late times ($z \lesssim 10$) all modes of interest have entered the horizon. You might think then, that the $y \gg 1$ limit of the Meszaros equation, which describes sub-horizon modes in the matter era, would apply. This is true if $\Omega_m = 1$. If the energy budget of the universe has another item at late times — either dark energy or curvature — then we must retrace the steps which led to the Meszaros equation. Before doing this, I want to point out that, no matter what constitutes the energy budget today, all modes will experience the same growth factor. We saw this in the previous section, where the Meszaros equation was independent of k. And we will soon see it again, when we generalize the Meszaros equation to account for other forms of energy. This uniform growth is a direct result of the fact that cold, dark matter has zero pressure. Therefore, once a mode enters the horizon, there is no way for pressure to smooth out the inhomogeneities and all modes evolve identically.

We want to derive an evolution equation analagous to the Meszaros equation, but allowing for the possibility of energy other than matter or radiation. We can take the $y \gg 1$ limit of Eqs. (7.54)–(7.56), but we must rethink the coefficient of the source term in the Poisson equation. Since radiation can be ignored, the coefficient multiplying δ in Eq. (7.56) is now $4\pi G\rho_{\rm dm} = (3/2)H_0^2\Omega_m a^{-3}$. Also when differentiating Eq. (7.54) previously, we set $(1/aHy)' = -(1+y)^{-1}(2aHy)^{-1}$; here we need to account for other contributions to H' so Eq. (7.57) becomes

$$\delta'' + ikv\left(\frac{d(aHy)^{-1}}{dy} - \frac{1}{aHy^2}\right) = \frac{3\Omega_m H_0^2}{2y^3 a^2 H^2 a_{\rm eq}}\delta. \tag{7.72}$$

Replacing the velocity term using the continuity equation as before leads to

$$\frac{d^2\delta}{da^2} + \left(\frac{d\ln(H)}{da} + \frac{3}{a}\right)\frac{d\delta}{da} - \frac{3\Omega_m H_0^2}{2a^5 H^2}\delta = 0. \tag{7.73}$$

Here I have divided by $a_{\rm eq}^2$ and we will now use a as the variable instead of y. In this large y limit, all factors of $a_{\rm eq}$ disappear.

There are two solutions to Eq. (7.73). One solution is $\delta \propto H$. It is easy to check this if all the energy is nonrelativistic matter, so that the solution is proportional to $a^{-3/2}$. Then all three terms scale as $a^{-7/2}$; the coefficient of the first is 15/4, the second $-9/4$, and the last 3/2. The sum of these does indeed vanish. In Exercise 7, you will be asked to show that $\delta \propto H$ is a solution if there are other components of energy in the universe. This solution is pretty, but it is not the one we want since almost all current models of the universe have a nonincreasing Hubble rate. The modes we are interested in — those that remain long after horizon crossing — are the growing modes. So we are interested in the other solution of Eq. (7.73).

To obtain the growing mode, we try a solution of the form $u = \delta/H$. The evolution equation for u then becomes

$$\frac{d^2u}{da^2} + 3\left[\frac{d\ln(H)}{da} + \frac{1}{a}\right]\frac{du}{da} = 0. \tag{7.74}$$

This first-order equation for u' can be integrated to obtain

$$\frac{du}{da} \propto (aH)^{-3}. \tag{7.75}$$

Integrating again and remembering that the second solution, the growth factor, is uH leads to an expression for the growth factor

$$D_1(a) \propto H(a)\int^a \frac{da'}{(a'H(a'))^3}. \tag{7.76}$$

I have glossed over the proportionality constant. This is fixed by the definition of Eq. (7.4), which says that, early on when matter still dominates (say at $z \simeq 10$), D_1 should be equal to a. At those times, $H = H_0\Omega_m^{1/2}a^{-3/2}$ so the growth factor is

$$D_1(a) = \frac{5\Omega_m}{2}\frac{H(a)}{H_0}\int_0^a \frac{da'}{(a'H(a')/H_0)^3}. \tag{7.77}$$

The growth factor in an open universe without dark energy can be computed analytically (see Exercise 8).

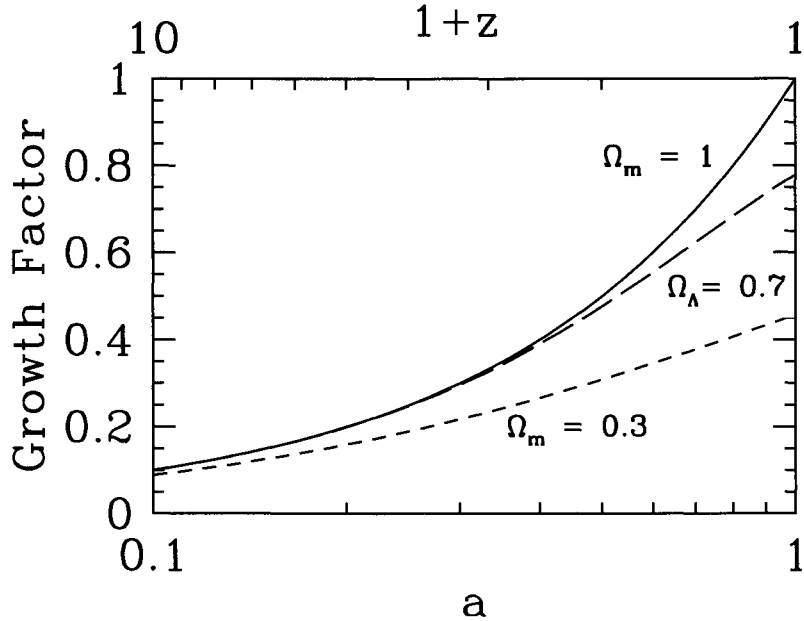

Figure 7.12. The growth factor in three cosmologies. Top two curves are for flat universes without and with a cosmological constant. Bottom curve is for an open universe.

Figure 7.12 shows the growth factor for three different cosmologies. As mentioned above, if the universe is flat and matter dominated, the growth factor is simply equal to the scale factor. In both open and dark energy cosmologies, though, growth is suppressed at late times. This leads to an important qualitative conclusion: structure in an open or dark energy universe developed much earlier than in a flat, matter-dominated universe. There has been relatively little evolution at recent times if the universe is open or dark energy-dominated. Therefore, whatever structure is observed today was likely in place at much earlier times. We will see some quantitative implications of this in Section 9.5.

7.6 BEYOND COLD DARK MATTER

There is more to the universe than just cold dark matter. Although CDM is the main component in most cosmological models, so that the transfer function we derived earlier is a good approximation to reality, there are trace amounts of other stuff. To be completely accurate we need to account for this other stuff. Here I

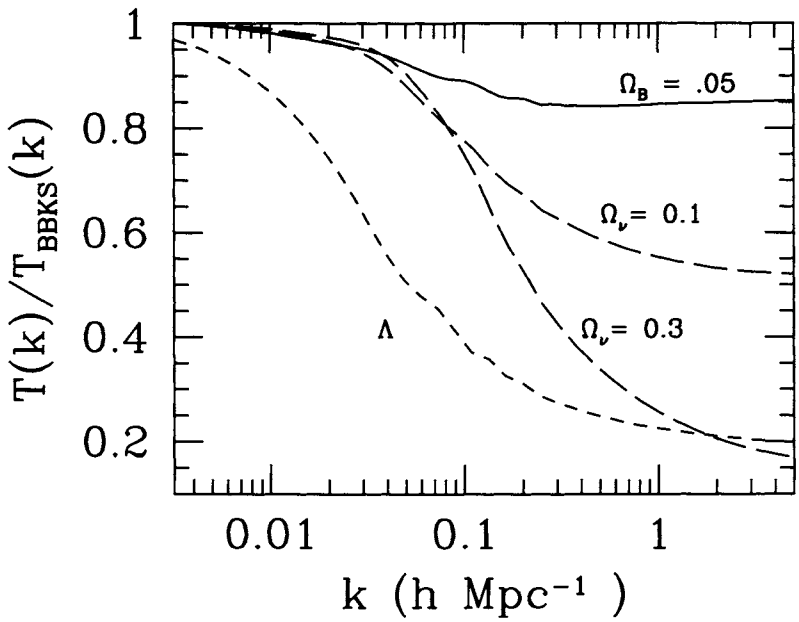

Figure 7.13. The ratio of the transfer function to the BBKS transfer function (Eq. (7.70)) which describes dark-matter-only (no baryons) perturbations. Top curve (and all other curves as well) has 5% baryons. Two middle curves show different values for a massive neutrino. Bottom curve has a cosmological constant $\Omega_\Lambda = 0.7$.

focus on three additional components. First, we consider the effect of the baryons, which constitute roughly 10% of the total matter in most models, on the transfer function. Then, we entertain the possibility that neutrinos have mass and examine the resultant effect on the transfer function. Finally, dark energy—one model for which is the cosmological constant—is considered.

Figure 7.13 shows the transfer functions accounting for these components. A realistic baryon fraction suppresses the transfer function on small scales. A massive neutrino does the same, with the nature and amplitude of the suppression depending on the neutrino mass. Dark energy, here in the form of a cosmological constant, moves the epoch of equality to later times, thereby reducing $k_{\rm eq}$. The break in the transfer function therefore comes on much larger scales than in the standard CDM model, in apparent agreement with the data exhibited in Figure 7.11.

7.6.1 Baryons

Baryons account for about 4% of the total energy density in the universe. As such, their effect on the matter power spectrum is small. A careful examination of Figure 7.13 reveals two signatures of a nonzero baryon density. The first is that the power spectrum is suppressed on small scales. This is not surprising: at early times, before decoupling, baryons are tightly coupled to photons. Therefore, just as radiation

perturbations decay when entering the horizon, so too do baryon overdensities. After decoupling, baryons are released from the relatively smooth radiation field and fall into the gravitational potentials set up by the dark matter. The depth of these wells is smaller than we estimated in Section 7.3, though, because only a fraction $\Omega_{\rm cdm}/\Omega_m$ of the total matter was involved in the collapse.

The second effect of baryons is less noticable in Figure 7.13 and indeed may never get measured in real life either. Nonetheless, it is extremely important if only because it hints at a fundamental feature of the radiation field. In all the curves in Figure 7.13, except the $\Omega_\nu = 0.3$ case, you can see small oscillations in the transfer function centered around $k \simeq 0.1\,h$ Mpc^{-1}. These are not numerical artifacts. Rather, they are manifestations of the oscillations that the combined baryon/photon fluid experience before decoupling. We got a glimpse of these in Section 7.3.2 (e.g., Figure 7.8) when we considered the potential in the radiation-dominated era. Just as the potential oscillates in this era, the baryon/photon fluid also oscillates. It is the traces of these oscillations that are imprinted on the matter transfer function. They are barely (if at all) detectable because baryons are such a small fraction of the total matter. In the baryon-only model plotted in Figure 1.13, the oscillations were much more noticeable.[5] And these oscillations are also prominent in the spectrum of the radiation perturbations, as we will see in the next chapter.

7.6.2 Massive Neutrinos

Neutrinos are known to exist, and the standard Big Bang model gives a definite prediction for how many there are in the universe (Eq. (2.77)). Massive neutrinos may play an important role in structure formation. Conversely, an accurate measurement of the power spectrum may enable us to infer neutrino masses. For orientation, recall the difference between massless (Eq. (2.78)) and massive (Eq. (2.80)) neutrino energy densities. The best bet from experiments is that the most massive neutrino has a mass of order 0.05 eV, therefore contributing $\Omega_\nu \simeq 10^{-3}$. Even this trace amount might eventually be detectable if the power spectrum can be measured accurately enough. There is also the possibility that one or more neutrinos has a larger mass (see the footnote on Page 46). Current upper limits from structure formation hover around 2 eV (Elgaroy *et al.*, 2002).

The reason why even a small admixture of massive neutrinos affects the power spectrum is that, especially if they are light, neutrinos can move fast (they are not *cold* dark matter) and stream out of high-density regions. Perturbations on scales smaller than the free-streaming scale are therefore suppressed. Indeed, a long time ago, cosmologists considered the possibility that all the dark matter in the universe was in the form of neutrinos. If this were so, then there would be no power on small scales and structure would have to form from the "top down."

We can estimate the scale on which perturbations are damped by computing the comoving distance a massive neutrino can travel in one Hubble time at equality.

[5] Incidentally, we now also understand why the power in Figure 1.13 is so low in the baryon-only universe: there is no dark matter which can cluster before recombination.

This calculation is trivial, however, if the neutrino mass is in the eV range. For then, the average velocity, T_ν/m_ν, is of order unity at equality. So neutrinos can freestream out of horizon-scale perturbations at equality. This leads to a suppression in power on all scales smaller than $k_{\rm eq}$.

Figure 7.13 shows this suppression. Note, though, that the effect is a little subtle. A lighter neutrino can free-stream out of larger scales, so the suppression begins at lower k for the $\Omega_\nu = 0.1$ mass than for the $\Omega_\nu = 0.3$ case. On the other hand, the more massive neutrino constitutes more of the total density so it suppresses small-scale power more than does the lighter neutrino.

7.6.3 Dark Energy

Cosmologists have recently accumulated tantalizing evidence for dark energy in the universe above and beyond the dark matter that we have spent so much time on in this chapter. If dark energy exists, how does it affect the matter perturbations?

The first effect of dark energy is indirect. Since theoretical prejudice and evidence both indicate that the universe is flat, $\Omega_{\rm de} \simeq 0.6$-$0.7$ implies that the matter density, Ω_m, is less than 1. This has a huge impact on the power spectrum, because we have seen that the power spectrum turns over at $k_{\rm eq}$, which is proportional to Ω_m. So dark energy leads to a turnover in the power spectrum on a scale much larger than predicted in standard CDM. In fact, as we saw in Figure 7.11, this is one of the pieces of evidence for dark energy. The turnover in the power spectrum does not appear on the scale predicted by standard CDM.

The second effect is again related to the smaller matter density in most models of dark energy. As a result of the Poisson equation (7.7), overdensities are inversely proportional to Ω_m for a fixed potential. Therefore, the amplitude of the power spectrum increases as the matter decreases, or equivalently in a flat universe as the dark energy content goes up. With a few caveats to be discussed in Chapter 8, large-angle CMB anisotropies fix the potential on large scales. When normalizing to these large-angle results, therefore, the power spectrum for a model with dark energy is normalized higher than one without.

The third effect of the dark energy on the density inhomogeneities is more direct and more model dependent. At late times, amplification of perturbations is controlled by the growth factor of Eq. (7.77). The evolution of the Hubble rate depends on the model of dark energy, so different models of dark energy predict different growth factors. If we parameterize the dark energy by its equation of state (2.84), then the Hubble rate in a flat universe evolves as

$$\frac{H(z)}{H_0} = \left[\frac{\Omega_m}{a^3} + \frac{\Omega_{\rm de}}{a^{3[1+w]}}\right]^{1/2} \tag{7.78}$$

at late times. Using this time dependence, it is straightforward to perform the integral in Eq. (7.77) and find the growth factor for a given equation of state (see Exercise 11).

To sum up, dark energy affects the power spectrum by changing $k_{\rm eq}$ and the normalization (this depends only on $\Omega_{\rm de}$) and by changing the growth factor at late times (depends on both $\Omega_{\rm de}$ and w). Careful observations of the matter spectrum therefore may enable us to learn about dark energy.

SUGGESTED READING

Once again *The Large Scale Structure of the Universe* (Peebles) is a useful reference. Since it was written before the implications of cold dark matter and inflation were explored, though, it does not contain a transfer function or power spectrum such as the ones we have derived (although Peebles himself was instrumental in computing these things several years after the book was published). A more up-to-date book, which is particularly strong on large-scale structure is *Structure Formation in the Universe* (Padmanabhan).

The first papers to work out the CDM transfer function are particularly instructive to read, not least because they also focus on some of the physical implications of the hierarchical theories. See Blumenthal *et al.* (1984) and Peebles (1982). The most important recent paper is Seljak and Zaldarriaga (1996), not so much because it contains a concise description of the set of coupled equations to be solved (although it does that), but because it makes available CMBFAST, a code which computes transfer functions and CMB anisotropy spectra. It is currently available at `http://physics.nyu.edu/matiasz/CMBFAST/cmbfast.html`. The treatment in this chapter follows most closely the small scale analytic solution of Hu and Sugiyama (1996), a paper which is extremely rich and well worth reading. A more recent paper by Eisenstein and Hu (1998) employs the analytic small-scale solution to derive accurate fitting formulae that move beyond those presented by Bardeen, Bond, Kaiser, and Szalay (1986, BBKS).

EXERCISES

Exercise 1. Derive Eqs. (7.11) and (7.12).
(a) First neglect the scattering term in Eq. (4.100), the one proportional to $\dot{\tau}$. Then the photon evolution equation is identical to the neutrino evolution equation (4.107). Show that this collisionless equation reduces to the two equations for the monopole and dipole. To get the monopole equation, multiply Eq. (4.107) by $(d\mu/2)\mathcal{P}_0(\mu) = d\mu/2$ and integrate from $\mu = -1$ to 1. To get the dipole, multiply by $(d\mu/2)\mathcal{P}_1(\mu)$ and integrate.
(b) Show that, in the limit of small baryon density, the scattering term in Eq. (4.100) can indeed be neglected. Neglect Π, since the quadrupole and polarization are very small. Then show that the scattering term is proportional to R, 3/4 times the baryon-to-photon ratio. You will want to use Eq. (4.106). It cannot be emphasized enough that this series of approximations is valid only for the purposes of this chapter, wherein we are interested in the matter distribution.

Exercise 2. Solve the set of five equations ((7.11)–(7.14) and (7.15)) numerically to obtain the transfer function for dark matter. Use the initial conditions derived in Chapter 6. The one numerical problem you may encounter using Eq. (7.15) occurs on small scales when you try to evolve all the way to the present. The photon moments then become difficult to track, and even a good differential equation solver

will balk at late times. However, there are several simple solutions to this: (i) by the late times in question, the potential is constant so there is no need to evolve all the way to the present or (ii) stop following the photon moments after a certain time; they don't have any effect on the matter distribution at late times anyway. Plot the transfer function for sCDM (with Hubble constant $h = 0.5$) and ΛCDM (with $\Omega_\Lambda = 0.7$ and $h = 0.7$). Compare with the BBKS transfer function of Eq. (7.70).

Exercise 3. The four subsections in Sections 7.2 and 7.3 correspond to four different approximations to the full set of Einstein–Boltzmann equations. In the following table, fill in the regime of validity for each approximation:

	$a \ll a_{\rm eq}$	$a \sim a_{\rm eq}$	$a \gg a_{\rm eq}$
$k\eta \ll 1$			
$k\eta \sim 1$			
$k\eta \gg 1$			

For example, the super-horizon solution of Section 7.2.1 is valid along the whole top row, since it sets $k\eta \to 0$. Note that time evolves from upper left to bottom right, so the fact that none of the approximations work in the center square means that only those scales that enter the horizon well before or well after equality will be subject to analytic techniques.

Exercise 4. Fill in some of the algebraic detail left out of Section 7.2.1.
(a) Show that Eq. (7.24) leads to Eq. (7.25) by carrying out the differentiation.
(b) Show that Eq. (7.25) is equivalent to Eq. (7.27) when the definition of u from Eq. (7.26) is used.
(c) Show that the integral in Eq. (7.31) can be done analytically with the result given in Eq. (7.32). One way to do the integral is to define a dummy variable $x \equiv \sqrt{1+y}$.

Exercise 5. Find the wavenumber of the mode which equals the inverse comoving Hubble radius at equality. That is, define $k_{\rm eq}$ to be equal to $a_{\rm eq}H(a_{\rm eq})$. Show that this definition implies

$$k_{\rm eq} = \sqrt{\frac{2\Omega_m H_0^2}{a_{\rm eq}}}. \tag{7.79}$$

Then use Eq. (2.87) to show that $k_{\rm eq}$ is given by Eq. (7.39). Show that if you define $k_{\rm eq}$ by setting it to $1/\eta_{\rm eq}$, you get a number 17% lower.

Exercise 6. Define a_H, the scale factor at which wavelength k equals the comoving Hubble radius, via $a_H H(a_H) \equiv k$. Express $a_H/a_{\rm eq}$ in terms of k and $k_{\rm eq}$. Show that in the limit $k \gg k_{\rm eq}$, this expression reduces to

$$\lim_{k \gg k_{\rm eq}} \frac{a_H}{a_{\rm eq}} = \frac{k_{\rm eq}}{\sqrt{2}k}. \tag{7.80}$$

Exercise 7. Show that $\delta \propto H$ is a solution to the evolution equation (7.73) if the universe is flat with a cosmological constant. You will need to use Eq. (1.2). Show also that the solution is valid if the universe has zero cosmological constant, but is open with $\Omega_m < 1$.

Exercise 8. Derive the growth factor for an open universe with $\Omega_m < 1$:

$$D_1(a, \Omega_m) = \frac{5\Omega_m}{2(1-\Omega_m)} \left[3\frac{\sqrt{1+x}}{x^{3/2}} \ln\left(\sqrt{1+x} - \sqrt{x}\right) + 1 + \frac{3}{x} \right] \tag{7.81}$$

where $x \equiv (1-\Omega_m)a/\Omega_m$. There may be easier ways to do this (e.g., you might want to check *The Large Scale Structure of the Universe*, Section 11), but I found it easiest to define a dummy variable $y \equiv \Omega_m/a$; write the integral of Eq. (7.77) as

$$\int_{\Omega_m/a}^{\infty} \frac{dy}{y^2(y+1-\Omega_m)^{3/2}} = 2 \left[\frac{d}{d\epsilon}\frac{d}{d\lambda} \int_{\Omega_m/a}^{\infty} \frac{dy}{(y+\epsilon)\sqrt{y+\lambda}} \right]_{\epsilon=0, \lambda=1-\Omega_m} ; \tag{7.82}$$

and then use 2.246 from Gradshteyn and Ryzhik.

Exercise 9. One popular way to characterize power on a particular scale is to compute the expected RMS overdensity in a sphere of radius R,

$$\sigma_R^2 \equiv \langle \delta_R^2(x) \rangle. \tag{7.83}$$

Here

$$\delta_R(\vec{x}) \equiv \int d^3x' \delta(\vec{x}') W_R(\vec{x} - \vec{x}') \tag{7.84}$$

where $W_R(x)$ is the *tophat* window function, equal to 1 for $x < R$ and 0 otherwise; the angular brackets denote the average over all space.

(a) By Fourier transforming, express σ_R in terms of an integral over the power spectrum.

(b) Use the BBKS transfer function to compute σ_8 ($R = 8\,h^{-1}$ Mpc) for a standard CDM model ($h = 0.5, n = 1, \Omega_m = 1$). We will see in Chapter 8 that COBE normalization for this model is

$$\delta_H = 1.9 \times 10^{-5}. \tag{7.85}$$

The value of σ_8 you find is yet another sign of the sickness of the model. For galaxies, σ_8 is known to be unity (or less, depending on galaxy type). A model with $\sigma_8 > 1$ then requires galaxies to be less clustered than the dark matter. Present models of galaxy formation suggest that this is unlikely. There are even direct measures of σ_8 of the mass (e.g., Section 9.5); these too constrain σ_8 to be less than one.

(c) In the same model, plot σ_R as a function of R. Since σ_R monotically increases, small scales tend to go nonlinear before large scales, the signature of a hierarchical model.

Exercise 10. Rewrite σ from Exercise 9 as

$$\sigma_R^2 = \int_0^\infty \frac{dk}{k} \Delta^2(k) \tilde{W}_R^2(k), \tag{7.86}$$

where $\tilde{W}_R$ is the Fourier tranform of the tophat window function and $\Delta^2 = d\sigma^2/d\ln(k)$ is the contribution to the variance per $\ln(k)$. A useful transition point is the value of k at which Δ exceeds 1. Scales larger than this are linear, while smaller scales have gone nonlinear. Find $k_{\rm nl}$ defined in this way for the sCDM model described in Exercise 9.

Exercise 11. Compute the growth factors in a universe with $\Omega_{\rm de} = 0.7, \Omega_m = 0.3$, and $w = -0.5$. Plot as a function of a. Compare with the cosmological constant model ($w = -1$) with the same $\Omega_{\rm de}, \Omega_m$.